Structure of the calcium dependent type 2 secretion pseudopilus

Aracelys Lopez-Castilla[1,5], Jenny-Lee Thomassin[2,5], Benjamin Bardiaux[3,5], Weili Zheng[4], Mangayarkarasi Nivaskumar[2], Xiong Yu[4], Michael Nilges[3], Edward H. Egelman[4], Nadia Izadi-Pruneyre[1,6], Olivera Francetic[2,6]

[6] Corresponding authors: Nadia Izadi-Pruneyre (nadia.izadi@pasteur.fr) and Olivera Francetic (ofrancet@pasteur.fr)

This PDF file includes:

Supplementary Figures 1-13

Supplementary Tables 1-3

Supplementary References

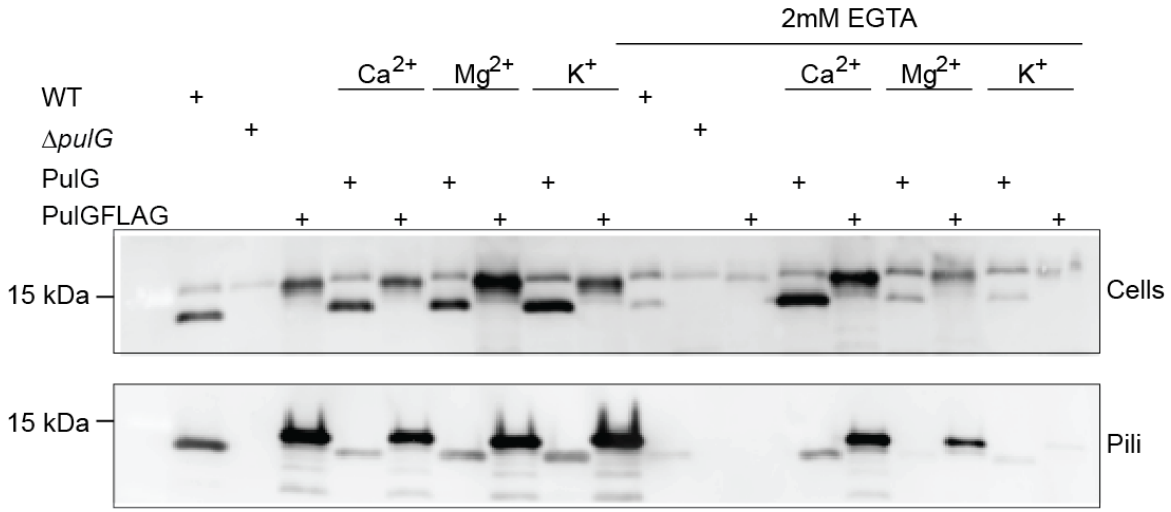

Supplementary Figure 1. Calcium efficiently restores PulG protein levels and piliation. E. coli strains producing the complete Pul T2SS (WT) or its derivatives lacking PulG *(ΔpulG*) and complemented with plasmids encoding PulG or PulG-FLAG variants were grown under pilus-inducing conditions in media supplemented with EGTA and/or indicated cations. Equivalent of 0.05 OD_{600nm} of cell- and pili fractions were resolved by Tris-Tricine SDS PAGE, transferred to a nitrocellulose membrane and probed with anti-PulG antibodies.

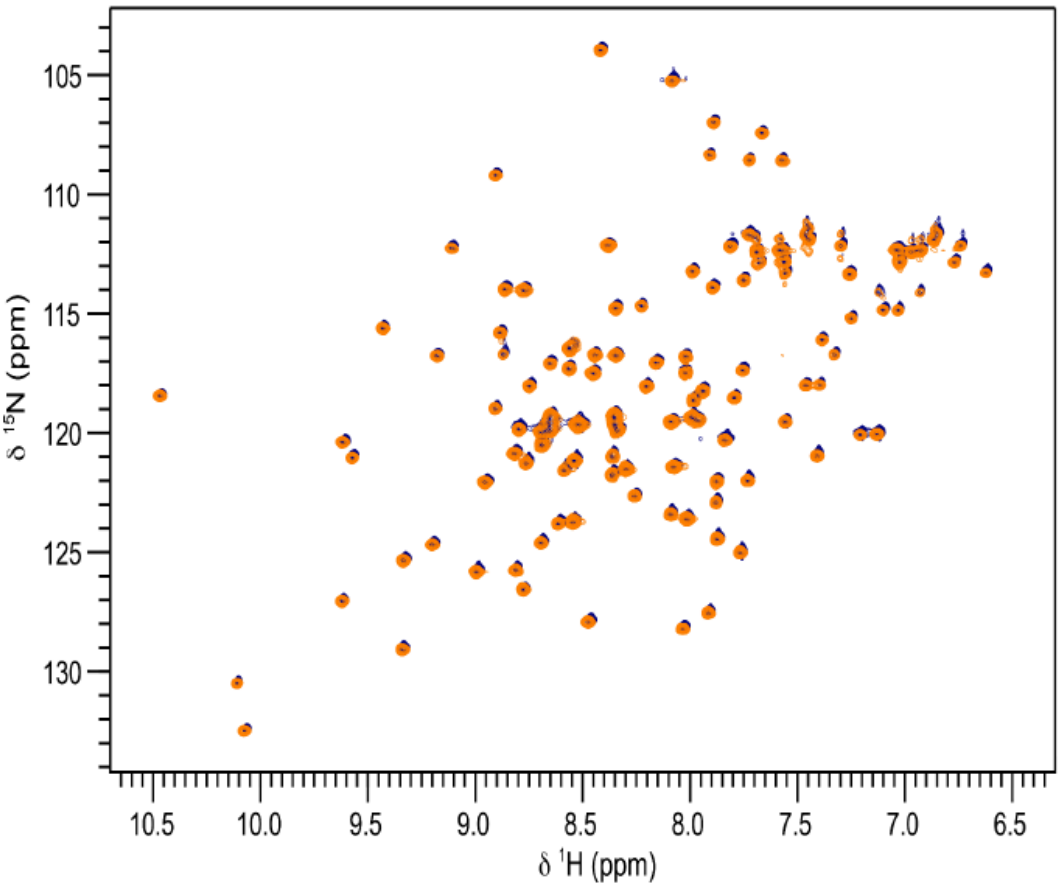

Supplementary Figure 2. PulGp native fold depends on the presence of calcium in a reversible manner. Superimposed ^{1}H-^{15}N HSQC spectra of 0.5 mM ^{15}N labelled-PulGp purified from the bacterial periplasm (blue contours) in 50 mM HEPES, 50 mM NaCl pH 7, and after adding 1 mM of calcium (orange contours) to the PulG-EGTA sample (Figure 2, red contours) after EGTA was removed.

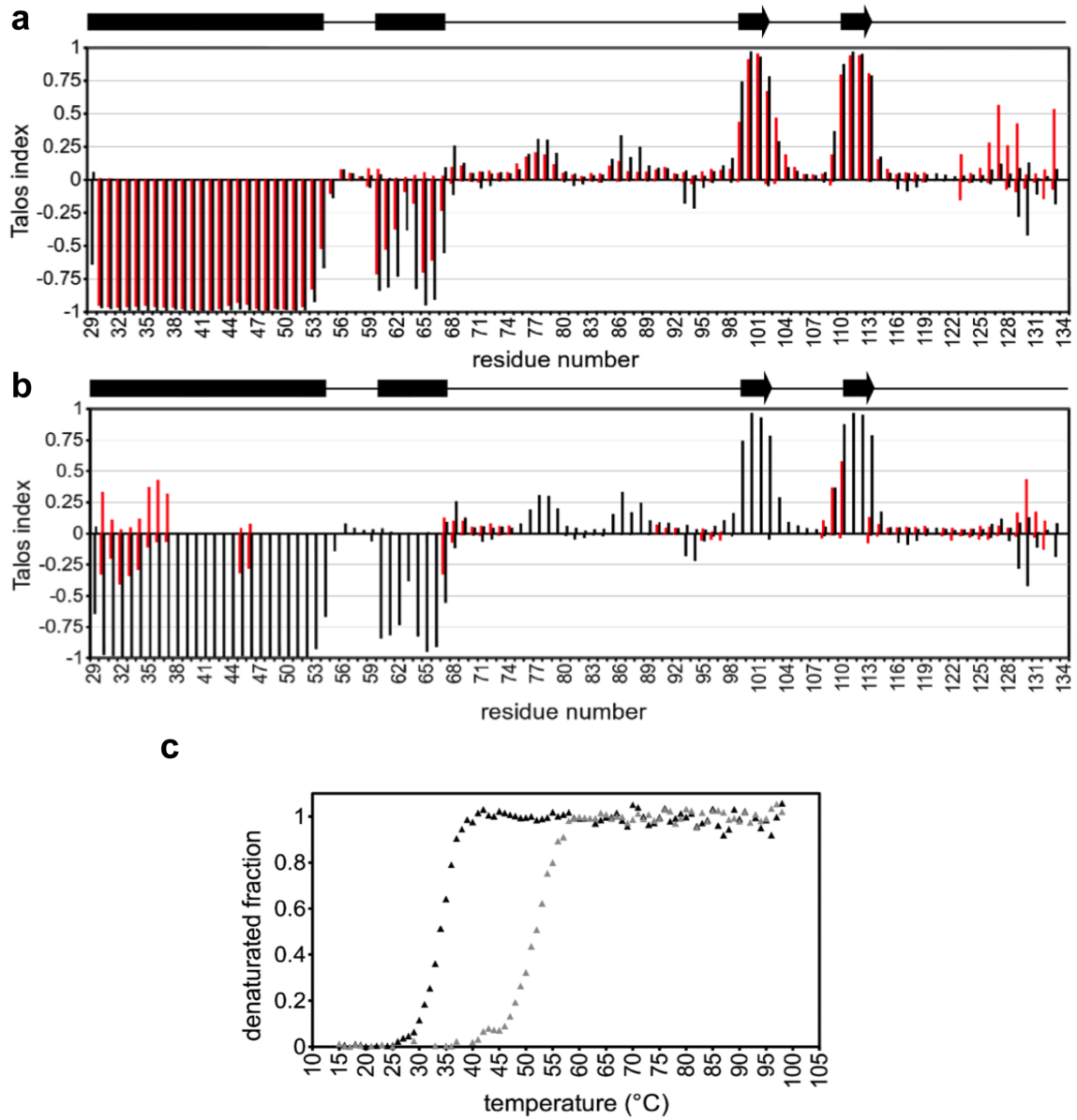

Supplementary Figure 3. Effect of calcium on structure and stability of PulGp. a and **b**, Secondary structure analysis of PulGp in the calcium-bound and free states based on the backbone resonances assignment. Talos index indicates TalosN probabilities for each residue to be involved in an α-helix (negative bars) or β-strand (positive bars). Black bars correspond to values obtained for PulGp in the presence of calcium and red bars indicate values obtained for the two conformers (**a** and **b**, respectively) in the calcium-free state. The predicted secondary structure of PulGp in the calcium-bound state is depicted on top (α-helix and β-strands are displayed as rectangles and arrows, respectively). **c,** PulGp thermo-stability is modulated by calcium. Normalized protein ellipticity curves (λ 222 nm) (measured in one experiment) of 50 µM PulGp in the presence of 1 mM of calcium or 1 mM of EGTA (grey and black triangles, respectively).

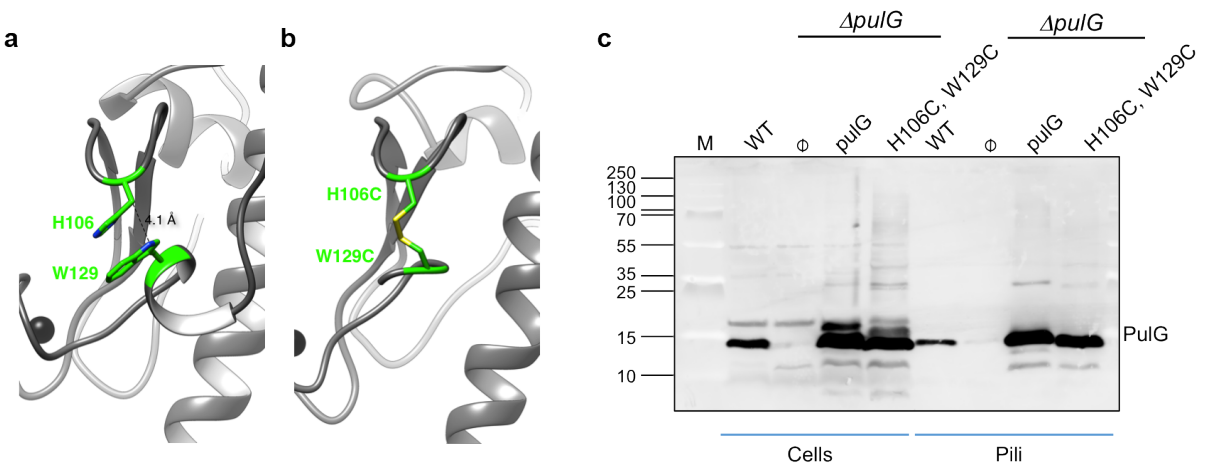

Supplementary Figure 4. Residues His106 and Trp129 (highlighted in green) are in close contact in the PulG monomer structure (**a**) and form an intra-molecular disulphide bond in variant PulG^{H106C,W129C} (PulG^{CC}) (**b**). **c**, *E. coli* strain PAP7460 harbouring plasmid pCHAP8185 (Supplementary Table 2) containing the complete set of *pul* T2SS genes (WT) or its *ΔpulG* derivative pCHAP8184 and either empty vector (⌀) or vector containing *pulG* or *pulG*^{CC} alleles were grown under pilus-inducing conditions in media supplemented with 2 mM $CaCl_2$. Cells were collected, normalized to OD of 1 and total extract from 0.05 OD_{600nm} of bacteria was analysed by Tris-Tricine SDS PAGE, transferred to a nitrocellulose membrane and probed with anti-PulG antibodies. M, molecular weight markers (in kDa) are indicated on the left. The figure is a representative of three experiments.

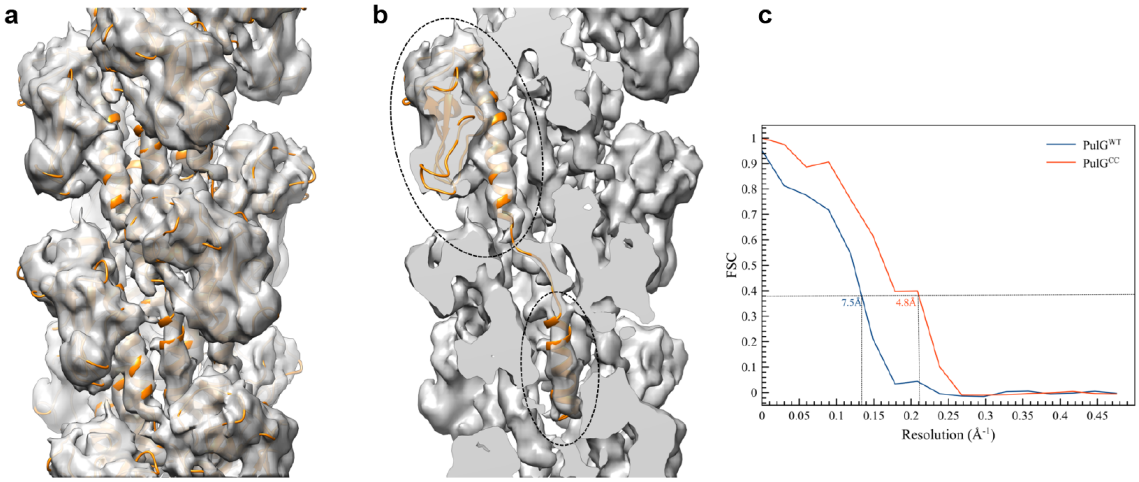

Supplementary Figure 5. The PulG^{CC} structure fitted in the PulG^{WT} cryo-EM reconstruction at ~7.5Å resolution. **a**, View from the outside of the pilus. **b**, Cross-section with a single PulG^{CC} subunit (PulGp and TMS helix are circled). **c**, Model-vs-map Fourier Shell Correlation (FSC) of the PulG^{CC} structure and the PulG^{CC} (red) or the PulG^{WT} (blue) cryo-EM maps. FSC of 0.38 (=√0.143) is achieved at resolution of 4.8 Å for PulG^{CC}, thus confirming the ~5 Å resolution. For PulG^{WT}, FSC of 0.38 corresponds to 7.5 Å resolution.

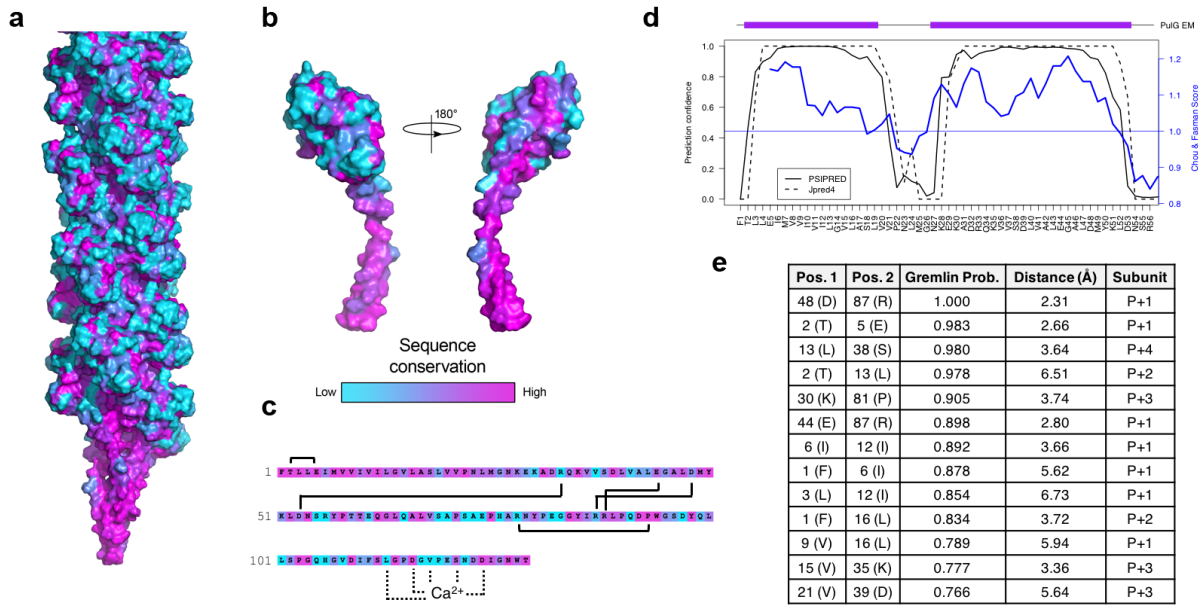

Pos. 1	Pos. 2	Gremlin Prob.	Distance (Å)	Subunit
48 (D)	87 (R)	1.000	2.31	P+1
2 (T)	5 (E)	0.983	2.66	P+1
13 (L)	38 (S)	0.980	3.64	P+4
2 (T)	13 (L)	0.978	6.51	P+2
30 (K)	81 (P)	0.905	3.74	P+3
44 (E)	87 (R)	0.898	2.80	P+1
6 (I)	12 (I)	0.892	3.66	P+1
1 (F)	6 (I)	0.878	5.62	P+1
3 (L)	12 (I)	0.854	6.73	P+1
1 (F)	16 (L)	0.834	3.72	P+2
9 (V)	16 (L)	0.789	5.94	P+1
15 (V)	35 (K)	0.777	3.36	P+3
21 (V)	39 (D)	0.766	5.64	P+3

Supplementary Figure 6. Sequence conservation of PulG shown on the PulG^{CC} pilus (**a**) and monomer (**b**) structure. Poorly conserved residues are shown in cyan while highly conserved positions are coloured in magenta. Residues at the surface of the pilus tend to be less conserved than buried ones. **c**, PulG sequence coloured by conservation. Stabilizing inter-subunit interactions in PulG^{CC} pilus are shown with continuous lines and calcium coordination with dotted lines. **d**, Prediction of helical propensity for residues 1 to 56 of PulG. Prediction confidence for being in helical conformation from PSIPRED (continuous line) [1] and Jpred4 (dotted line) [2] are show in black lines. Average score over a 5 a.a. window using the Chou & Fasman scale [3] for helical propensity is shown in blue line. The alpha-helical segments of the PulG^{CC} cryo-EM structure are shown on top (purple). **e**, Table of inter-subunit contacts in PulG^{CC} pilus structure (< 7Å) predicted by co-evolutionary analysis with Gremlin (Probability > 0.7) [4].

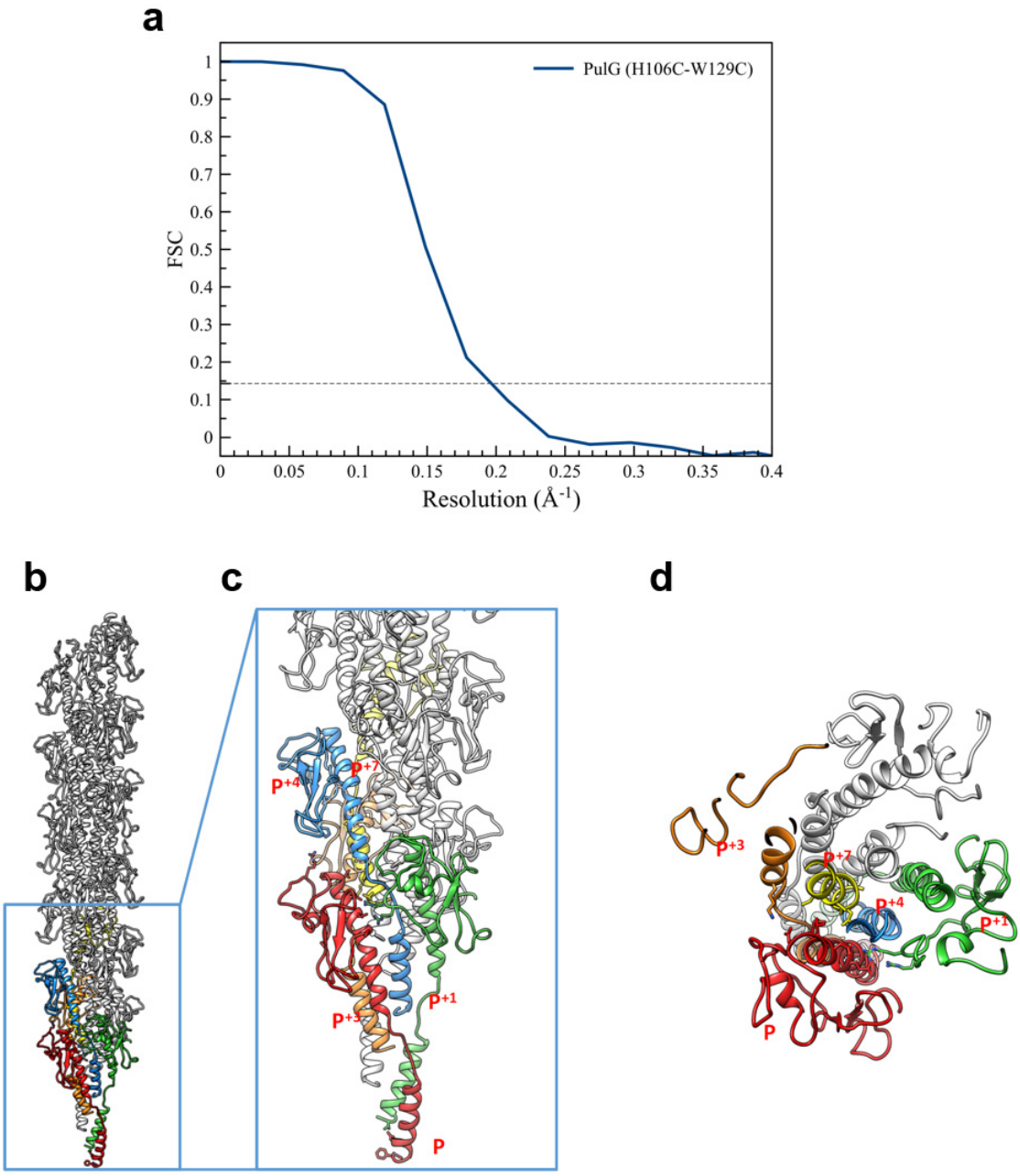

Supplementary Figure 7. **a**, The FSC between two independent half maps for pseudopilus PulG^{CC}, each generated from two non-overlapping data sets and reconstructed separately, shows a resolution ~5 Å at FSC =0.143. **b**, Ribbon representation of PulG^{CC} pseudopilus model, **c**, close-up view and **d**, top view are shown to illustrate the interaction network between protomer P (coloured in red) and the adjacent subunits (P_{+1}, green; P_{+3}, orange; P_{+4}, blue; P_{+7}, yellow). Besides making numerous contacts with P_{+1}, P_{+3} and P_{+4}, protomer P also forms hydrophobic contacts with P_{+1}, P_{+3} , P_{+4} and P_{+7} through the N-terminal α-helices.

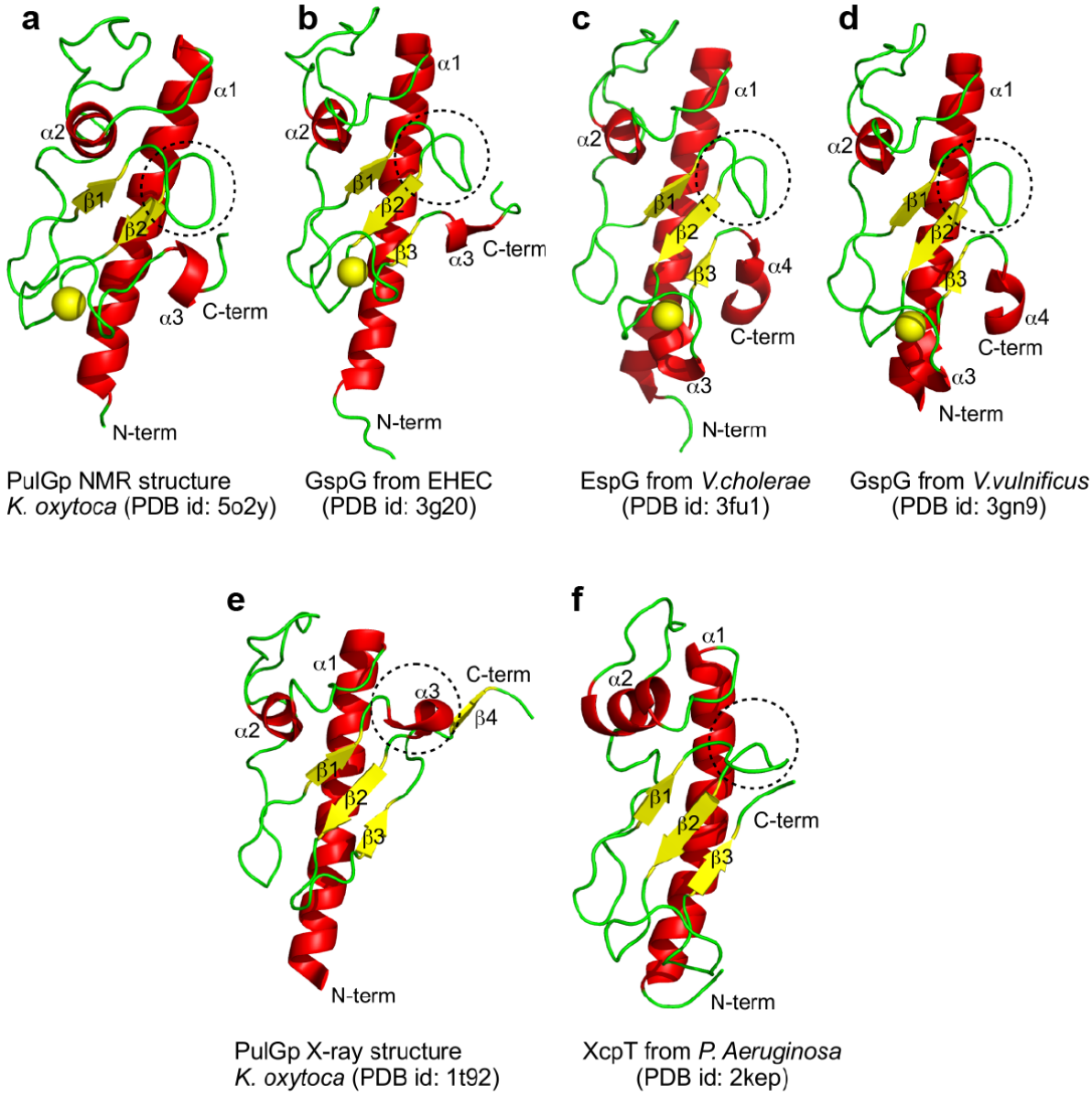

Supplementary Figure 8. Comparison of PulGp NMR structure (**a**) with its X-ray counterpart (**e**) [5] and with other major pseudopilins: GspG from enterohaemorrhagic *E. coli* (EHEC) (**b**), EspG from *Vibrio cholerae* (**c**), GspG from *Vibrio vulnificus* (**d**) [6] and XcpT from *Pseudomonas aeruginosa* (**f**) [7]. Helices are depicted in red, loops in green and β-strands in yellow. Calcium atoms are represented as yellow spheres and dashed circles indicate the β1-β2 loop.

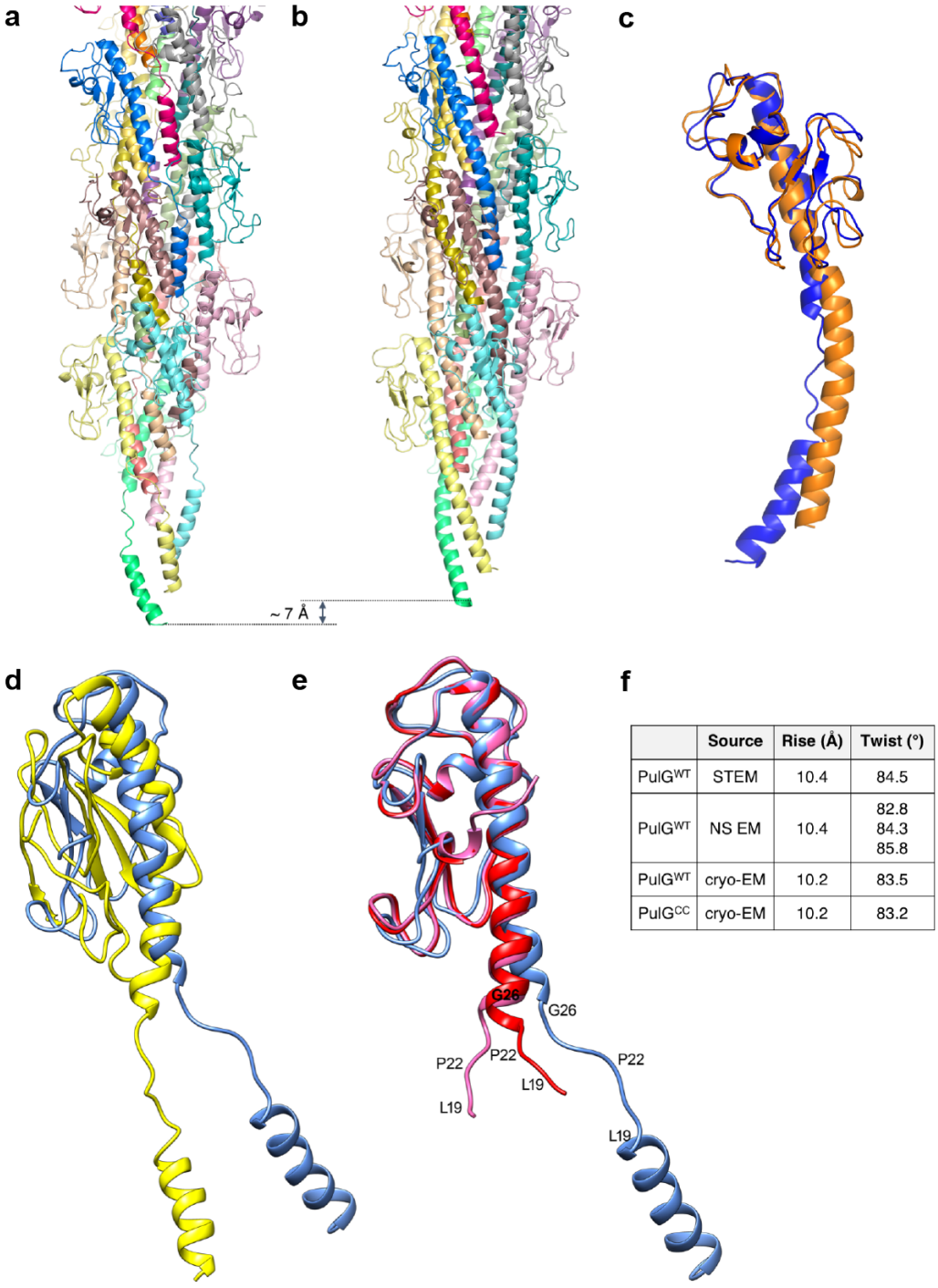

	Source	Rise (Å)	Twist (°)
PulG^{WT}	STEM	10.4	84.5
PulG^{WT}	NS EM	10.4	82.8 84.3 85.8
PulG^{WT}	cryo-EM	10.2	83.5
PulG^{CC}	cryo-EM	10.2	83.2

Supplementary Figure 9. Comparison of PulG^{CC} cryoEM structure (**a**) with PulG^{WT} pseudopilus model of Campos *et al*. [8] in **b**. **c**, Superposition of PulG monomers from PulG^{CC} cryo-EM structure (blue) and PulG^{WT} model (gold). Residues of the PulGp region (27 to 130) were used for superposition. **d**, Superposition of a monomer from the PulG^{CC} cryo-EM structure (blue) with a monomer from the *Neisseria meningitidis* T4P (yellow) cryo-EM structure (PDB 5KUA). **e**, Superposition of a monomer from the PulG^{CC} cryo-EM structure (blue) with the 2 subunits (red and pink) in the asymmetric unit of EHEC GspG X-ray structure (PDB 3G20). **f**, Helical symmetry parameters (rise and twist angle) of PulG^{WT} and PulG$^{H106C\text{-}W129C}$ (PulG^{CC}) pili determined by electron microscopy.

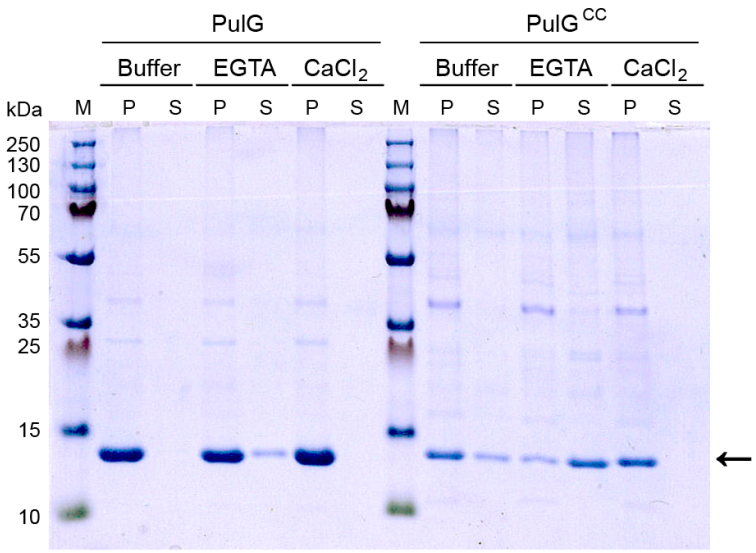

Supplementary Figure 10. Effect of calcium on disassembly of native PulG- and PulG^{CC} pili. Pseudopili present on the surface of PAP7460 cells harbouring pCHAP8184 and pCHAP8658 (PulG) or pCHAP8184 and pMS148 (PulG^{CC}) were mechanically sheared and isolated by ultracentrifugation. After purification, pseudopili were incubated in buffer alone or buffer supplemented with EGTA or $CaCl_2$ for 1.5 h and intact pseudopili (P) were separated from the supernatant containing broken or degraded pseudopili (S) by ultracentrifugation. The arrow indicates the position of PulG monomers. A representative of three independent experiments is shown.

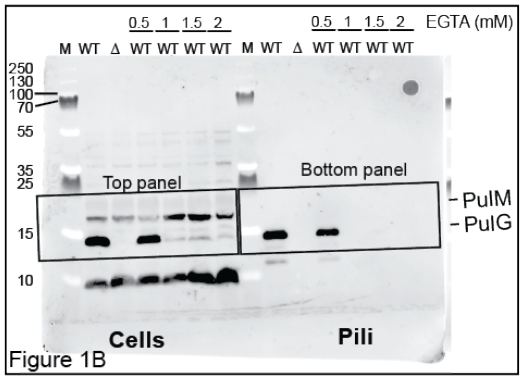

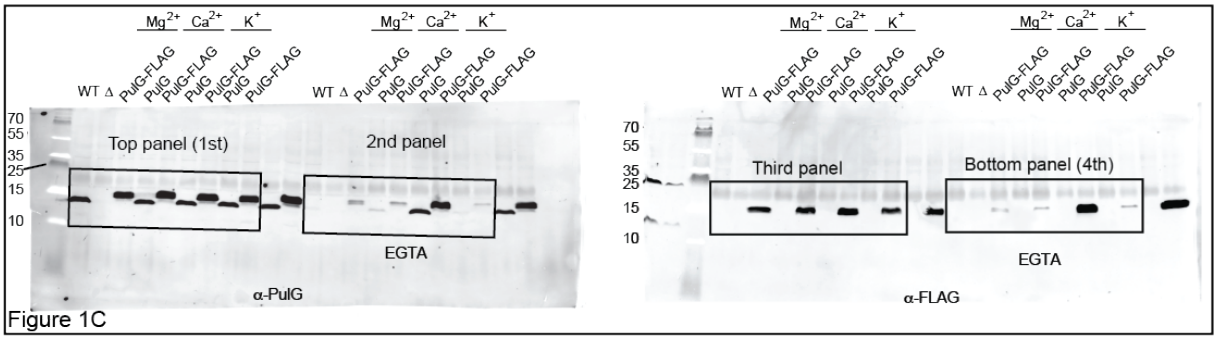

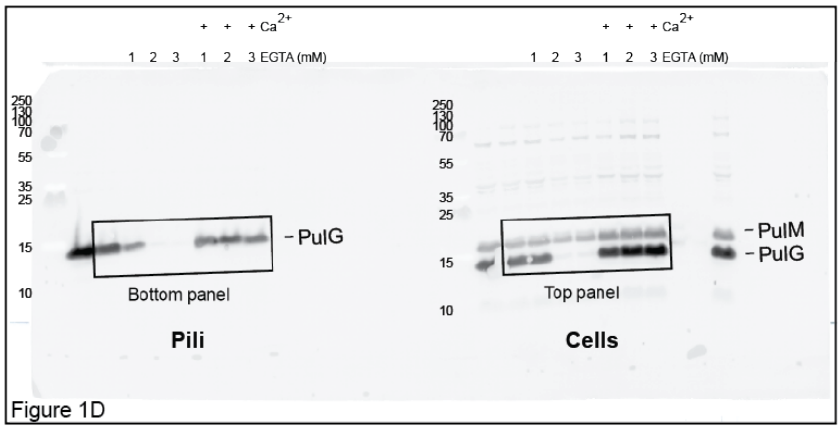

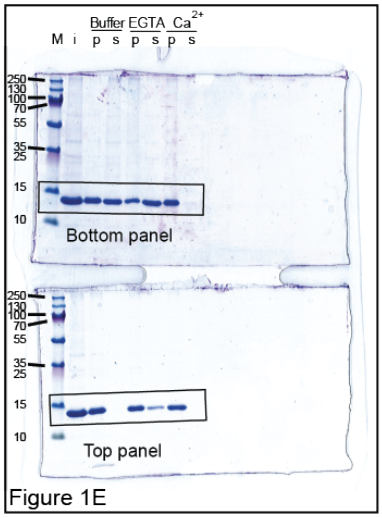

Supplementary Figure 11. Uncropped blots and gel shown in Figure 1.

a

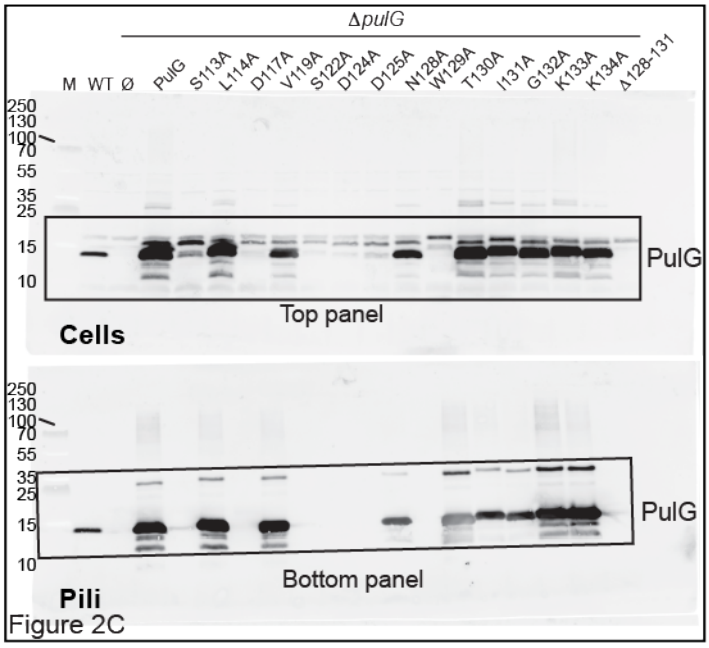

b

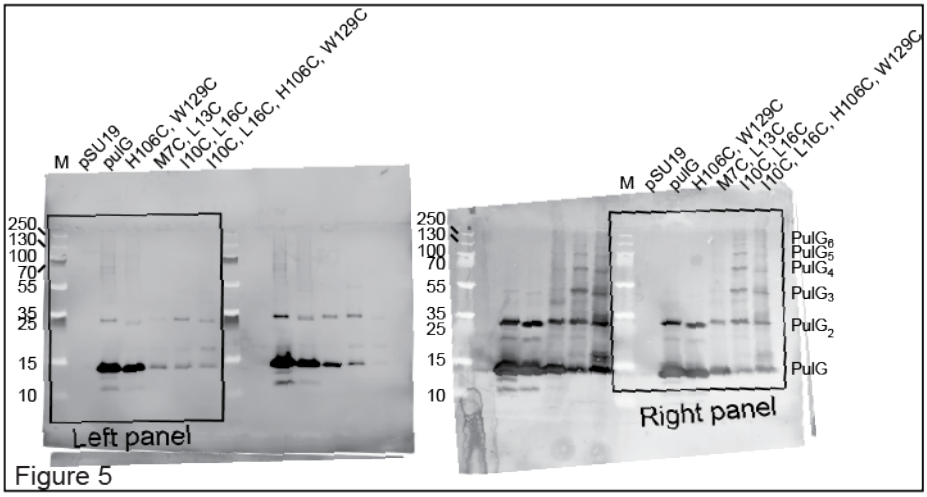

Supplementary Figure 12. Uncropped blots shown in Figure 2C (**a**) and Figure 5 (**b**).

a

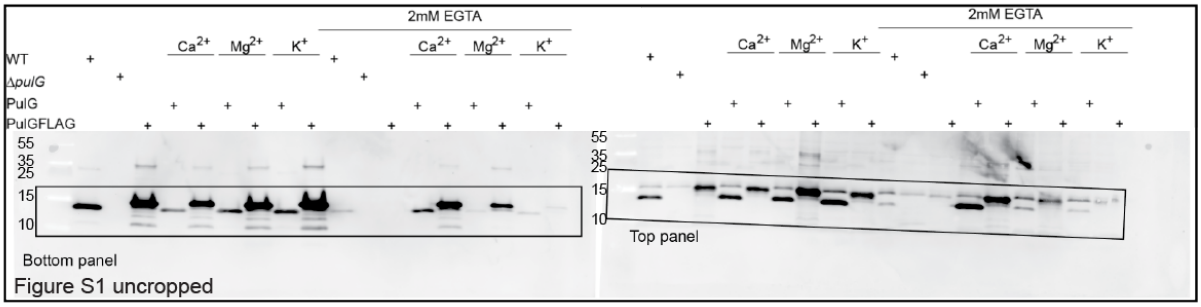

b

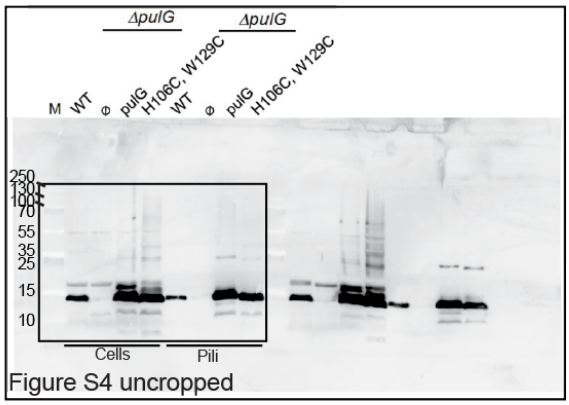

c

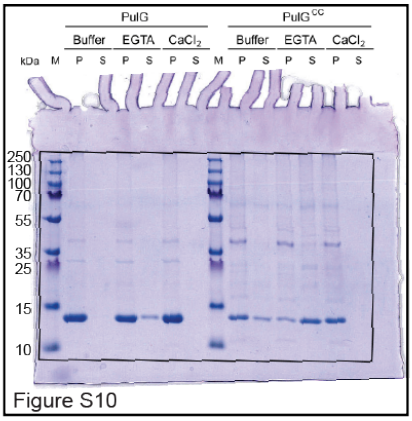

Supplementary Figure 13. Uncropped blots and gel shown in Supplementary Figure 1 (**a**), Supplementary Figure 4 (**b**) and Supplementary Figure 10 (**c**).

Supplementary Table 1. PulGp NMR structure statistics and restraints

A. Number of restraints	
NOE distance restraints	
Intra-residual (|i-j| = 0)	663
Sequential (|i-j| = 1)	412
Medium-range (2 ≤ |i-j| < 5)	304
Long-range (|i-j| ≥ 5)	397
Ambiguous	463
Total	2239
Hydrogen bonds restraints	44
Dihedral angles restraints (phi /psi)	156 (78 /78)
B. Restraints violation	
RMS of distance violations	
NOEs restraints (Å)	0.01
H-bonds restraints (Å)	0.02
RMS of dihedral angles (^{o})	0.90
C. Deviation from ideal geometry	
RMS for bond lengths (Å)	0.003
RMS for bond angles (^{o})	0.488
RMS for impropers (^{o})	1.353
D. Ramachandran statistics from Procheck (%)[a,b]	
Most favored regions	94.7
Allowed regions	5
Generously disallowed regions	0.1
Disallowed regions	0.2
E. RMSD from average structure (Å)[a]	
backbone atoms (Å)	0.50
heavy atoms(Å)	0.96
F. Global quality scores (raw/Z score)[a,b]	
Verify3D	0.3/ -2.57
ProsaII	0.39/ -1.08
Procheck (phi - psi)	0.01/ 0.35
Procheck (all)	-0.14/ -0.83
MolProbity clash score	20.20/ -1.94

[a] for ordered residues: 29-123, 126-131, selected based on dihedral order parameter phi+psi>1.8.
[b] computed using the PSVS server.

Supplementary Table 2. Bacterial strains, plasmids and oligonucleotides.

***E. coli* strain**	**Genotype**			**Source**
DH5α	F⁻ Φ80*lacZΔM15 Δ*(*lacZYA-argF*) *U169 recA1 endA1 hsdR17* (r_K–, m_K+) *pho*A *supE44* λ⁻ *thi-1 gyrA96 relA1*			Laboratory collection
PAP 7460	*Δ(lac-argF)U169 araD139 relA1 rps150 ΔmalE444 malG501* F′ *lacI*^{Q}Tn*10*			[9]
BL21 (DE3)	*fhuA2 [lon] ompT gal (λ DE3) [dcm] ΔhsdS* *λ DE3 = λ sBamHIo ΔEcoRI-B int::(lacI::placUV5::T7 gene1) i21 Δnin5*			Laboratory collection
Plasmid	**Origin/ resistance**[a]	**Markers**	**Primers used to generate plasmid**[b,c]	**Source**
pSU19	p15A/Cm	p*lacZ, lacZ′*		[10]
pCHAP 7354	p15A/Cm	pSU19 containing *pulG*(I10C, L16C)		[8]
pCHAP 7614	p15A/Cm	pSU19 containing *pulG*(M7C, L13C)		[8]
pCHAP 8184	ColE1/Ap	pCHAP8185 Δ*pulG*		[8]
pCHAP 8185	ColE1/Ap	*pulS, pulA*$_{NA}$*, pulB, pulCDEFGHIJKLMNO*		[11]
pCHAP 8658	p15A/Cm	pSU19 containing *pulG*		[12]
pMS113	p15A/Cm	pSU19 containing *pulG*(D117A)	ctccggcacgcccgcgggcccgaggctg cagcctcgggcccgcgggcgtgccggag	This study
pMS114	p15A/Cm	pSU19 containing *pulG*(D124A)	cttcccgatcgtccaattgccgatatcggcattgctctc gagagcaatgccgatatcggcaattggacgatcgggaag	This study
pMS115	p15A/Cm	pSU19 containing *pulG*(D125A)	gagagcaatgacgctatcggcaactggacg cgtccagttgccgatagcgtcattgctctc	This study
pMS134	p15A/Cm	pSU19 containing *pulG*(S113A)	gtccggcccgagggcgaaaatatccacctgac gtcaggtggatattttcgccctcgggccggac	This study
pMS135	p15A/Cm	pSU19 containing *pulG*(L114A)	ggtggatattttcagcgccgggccggacggcg cgccgtccggcccggcgctgaaaatatccacc	This study
pMS136	p15A/Cm	pSU19 containing *pulG*(V119A)	tgctctccggcgcgccgtccggc gccggacggcgcgccggagagca	This study
pMS137	p15A/Cm	pSU19 containing *pulG*(S122A)	gacggcgtgccggaggccaatgacgatatcgg ccgatatcgtcattggcctccggcacgccgtc	This study
pMS138	p15A/Cm	pSU19 containing *pulG*(N128A)	gagcaatgacgatatcggcgcttggacgatcgggaagaaa tttcttcccgatcgtccaagcgccgatatcgtcattgctc	This study
pMS139	p15A/Cm	pSU19 containing *pulG*(W129A)	gcaatgacgatatcggcaatgcgacgatcgggaagaaata tatttcttcccgatcgtcgcattgccgatatcgtcattgc	This study
pMS140	p15A/Cm	pSU19 containing *pulG*(T130A)	gcaatgacgatatcggcaattgtacgatcgggaagaaata tatttcttcccgatcgtacaattgccgatatcgtcattgc	This study
pMS141	p15A/Cm	pSU19 containing *pulG*(I131A)	acgatatcggcaattgggcgatcgggaagaaatag ctatttcttcccgatcgcccaattgccgatatcgt	This study
pMS142	p15A/Cm	pSU19 containing *pulG*(G132A)	cgatatcggcaattggacggccgggaagaaatagtgcgac gtcgcactatttcttcccggccgtccaattgccgatatcg	This study
pMS143	p15A/Cm	pSU19 containing *pulG*(K133A)	ggcaattggacgatcgcgaagaaatagtgcgac gtcgcactatttcttcgcgatcgtccaattgcc	This study
pMS144	p15A/Cm	pSU19 containing *pulG*(K134A)	gcaattggacgatcggggcgaaatagtgcgacagcg cgctgtcgcactatttcgccccgatcgtccaattgc	This study
pMS145	p15A/Cm	pSU19 containing *pulG*(Δaa128-131)	ttggacgatcgggaaggcatagtgcgacagcgcg cgcgctgtcgcactatgccttcccgatcgtccaa	This study

pMS146	p15A/Cm	pSU19 containing *pulG*(H106C)	tcgcactatttcttcccgccgatatcgtcattgc gcaatgacgatatcggcgggaagaaatagtgcga	This study
pMS148	p15A/Cm	pSU19 containing *pulG*(H106C, W129C)	gcaatgacgatatcggcaattgtacgatcgggaagaaata tatttcttcccgatcgtacaattgccgatatcgtcattgc	This study
pMS161	p15A/Cm	pSU19 containing *pulG*(I10C, H106C, W129C)	catggtggtgtgcgttatcctcggcgtg cacgccgaggataacgcacaccaccatg	This study
pMS162	p15A/Cm	pSU19 *placZ* driving *pulG*(I10C, L16C, H106C, W129C)	cctcggcgtgtgcgcaagcctcgtggtg caccacgaggcttgcgcacacgccgagg	This study
pQE30	ColE1/Ap	Vector N-terminal His_6 tag		Qiagen
pMS152	ColE1/Ap	pQE30 containing His_6-m*pulG*	cgggatccttcaccttactggaaatcatg gggaagctttgattactatttcttcccgatcgtcc	This study
pET20b+	ColE1/Ap	Expression vector N-terminal PelB signal peptide		Novagen
pMS153	ColE1/Ap	pET20b+ containing His_6-m*pulG*		This study
pMS155	ColE1/Ap	pET20b+ containing His_6-TEV-*pulGp*	cttccagggcatgggcaacaaggaaaaggc tacaggttctcgtgatggtgatggtgatgatcc	This study

[a]Ap (amplicillin); Cm (Chloramphenicol)
[b]Blank when no primers used
[c]Restriction sites are underlined

Supplementary Table 3. Refinement statistics of the PulG^{CC} pilus structure

Deviation from ideal geometry	
RMS[a] for bond lengths (Å)	0.015
RMS for bond angles (^{o})	1.52
Cβ deviations (%)	0.0
Molprobity statistics	
Ramachandran favoured (%)	86.5
Ramachandran allowed (%)	13.5
Ramachandran outliers (%)	0.0
Rotamer outliers (%)	0.0
Clashscore	9.09
Overall score	2.12

[a] RMS, root mean square

Supplementary References

1. Jones, D.T. Protein secondary structure prediction based on position-specific scoring matrices. *J. Mol. Biol.* **292**, 195-202 (1999).
2. Drozdetskiy, A., Cole, C., Procter, J. & Barton, G.J. JPred4: a protein secondary structure prediction server. *Nucleic Acids Res.* **43**, W389-94 (2015).
3. Chou, P.Y. & Fasman, G.D. Prediction of the secondary structure of proteins from their amino acid sequence. *Adv. Enzymol. Relat. Areas Mol. Biol.* **47**, 45-148 (1978).
4. Kamisetty, H., Ovchinnikov, S. & Baker, D. Assessing the utility of coevolution-based residue-residue contact predictions in a sequence- and structure-rich era. *Proc. Natl. Acad. Sci. USA* **110**, 15674-9 (2013).
5. Kohler, R. *et al*. Structure and assembly of the pseudopilin PulG. *Mol. Microbiol.* **54**, 647-64 (2004).
6. Korotkov, K.V. *et al*. Calcium is essential for the major pseudopilin in the type 2 secretion system. *J. Biol. Chem.* **284**, 25466-70 (2009).
7. Alphonse, S. *et al.* Structure of the *Pseudomonas aeruginosa* XcpT pseudopilin, a major component of the type II secretion system. *J. Struct. Biol.* **169**, 75-80 (2010).
8. Campos, M., Nilges, M., Cisneros, D.A. & Francetic, O. Detailed structural and assembly model of the type II secretion pilus from sparse data. *Proc. Natl. Acad. Sci. USA* **107**, 13081-6 (2010).
9. Possot, O.M., Vignon, G., Bomchil, N., Ebel, F. & Pugsley, A.P. Multiple interactions between pullulanase secreton components involved in stabilization and cytoplasmic membrane association of PulE. *J. Bacteriol.* **182**, 2142-52 (2000).
10. Bartolome, B., Jubete, Y., Martinez, E. & de la Cruz, F. Construction and properties of a family of pACYC184-derived cloning vectors compatible with pBR322 and its derivatives. *Gene* **102**, 75-8 (1991).
11. Cisneros, D.A., Bond, P.J., Pugsley, A.P., Campos, M. & Francetic, O. Minor pseudopilin self-assembly primes type II secretion pseudopilus elongation. *EMBO J.* **31**, 1041-53 (2012).
12. Nivaskumar, M. *et al.* Distinct docking and stabilization steps of the pseudopilus conformational transition path suggest rotational assembly of type IV pilus-like fibers. *Structure* **22**, 685-96 (2014).